

Ultrafast μ LIBS Imaging for the multiscale mineralogical characterization of pegmatite Rocks.

C. Alvarez-Llamas^a, A. Tercier^{a,b}, C. Ballouard^c, C. Fabre^c, S. Hermelin^{a,d}, J. Margueritat^a, L. Duponchel^e, C. Dujardin^{a,f}, V. Motto-Ros^{a,b*}.

Supplementary Material

Table of contents

1. Table 1. List of found elements on the different spectral ranges, showing some emission lines present in the spectra.
2. Figure SP 1. Amendra Sample Elemental maps for Mg, Rb, Na, Ca, Sr, Zn, Zr, Fe, Cu, P, Mn and Ti
3. Figure SP 2. Variability of the predicted pixel percentage relative to the mean (set to 1) with respect to the number of pixels attributed to each mineral phase independently.

^a Institut Lumière Matière (iLM), UMR5306, UCBL-CNRS; 10 Ada Byron; 69622 Villeurbanne, France

^b ABLATOM S.A.S., 5 rue de la Doua, 69100 Villeurbanne, France.

^c GeoRessources, UMR7356, Université de Lorraine-CNRS, F-54500 Vandoeuvre-lès-Nancy, France.

^d Laboratoire de Physique, ENS, Lyon, 46 allée d'Italie, 69007 Lyon, France

^e Laboratoire de Spectroscopie pour les Interactions, la Réactivité et L'Environnement, CNRS UMR 8516, Université de Lille, Villeneuve D'Ascq, France

^f Institut Universitaire de France (IUF), 75231 Paris, France

Table SP 1. List of found elements on the different spectral ranges, showing some emission lines present in the spectra.

Element		Lines Range 1 (nm)	Lines Range 2 (nm)	Lines Range 3 (nm)	Lines Range 4 (nm)
Al	Al I	308.22 309.28			
Ar	Ar I				696.54 706.72 738.40 750.39 763.51 794.81 811.53 801.57
B	B I	249.68 249.77			
Be	Be I	249.47 265.06		332.13	
	Be II		313.04		
C	C I	247.86			
Ca	Ca II		315.89 317.93		714.82 732.51
Cs	Cs I				807.9
Cu	Cu I			324.75 327.40	
Dy	Dy II			353.50 353.60	
Fe	Fe I	249.06 271.90	296.69 299.44 302.06 304.76	344.06 357.01 358.12	
	Fe II	259.94 275.57			
F	F I				865.6
Gd	Gd II			335.86 336.22 346.40	
K	K I				766.45 769.90
La	La II			330.31 333.75 334.46 338.09	
Li	Li I				678.78
Mg	Mg I	285.21			
	Mg II	279.55 280.27			
Mn	Mn II	257.61 259.37 260.57	293.31 293.93 294.92		
	Mn I			344.20 354.80 356.98	
Na	Na I				819.48
Nb	Nb II		292.78 294.15 309.41 313.08 316.34	322.55	
	Nb I			334.90 335.84 358.03	666.08 704.68 715.94
Ni	Ni I			341.47 344.63 345.85 346.16 356.64	
O	O I				777.42
P	P I	253.33 255.56			
Rb	Rb I				780.03
Si	Si I	251.61 252.41 252.85	288.16		
Sn	Sn I	242.17 242.95 257.16 270.65	284.0 286.33 300.91 303.41 317.50	326.23	
Sr	Sr II			338.07 346.45 347.49	
Ta	Ta II	249.43 263.55 267.59	282.75 284.45		
Th	Th II		283.23 283.72 306.77 318.82	325.63 326.27 340.27 346.99	
Ti	Ti II			323.45 324.20 334.94 336.12 337.15 338.38	
V	V II			326.77 327.11 327.61 351.73 354.52 355.68	
Y	Y II			320.03 320.33 321.67 334.23 332.79 354.90	
Yb	Yb II			328.94	
Zn	Zn I			328.23 330.26 334.50	
Zr	Zr II	254.14 272.26 272.64 273.27		339.20 343.82 349.61 350.57 355.66	

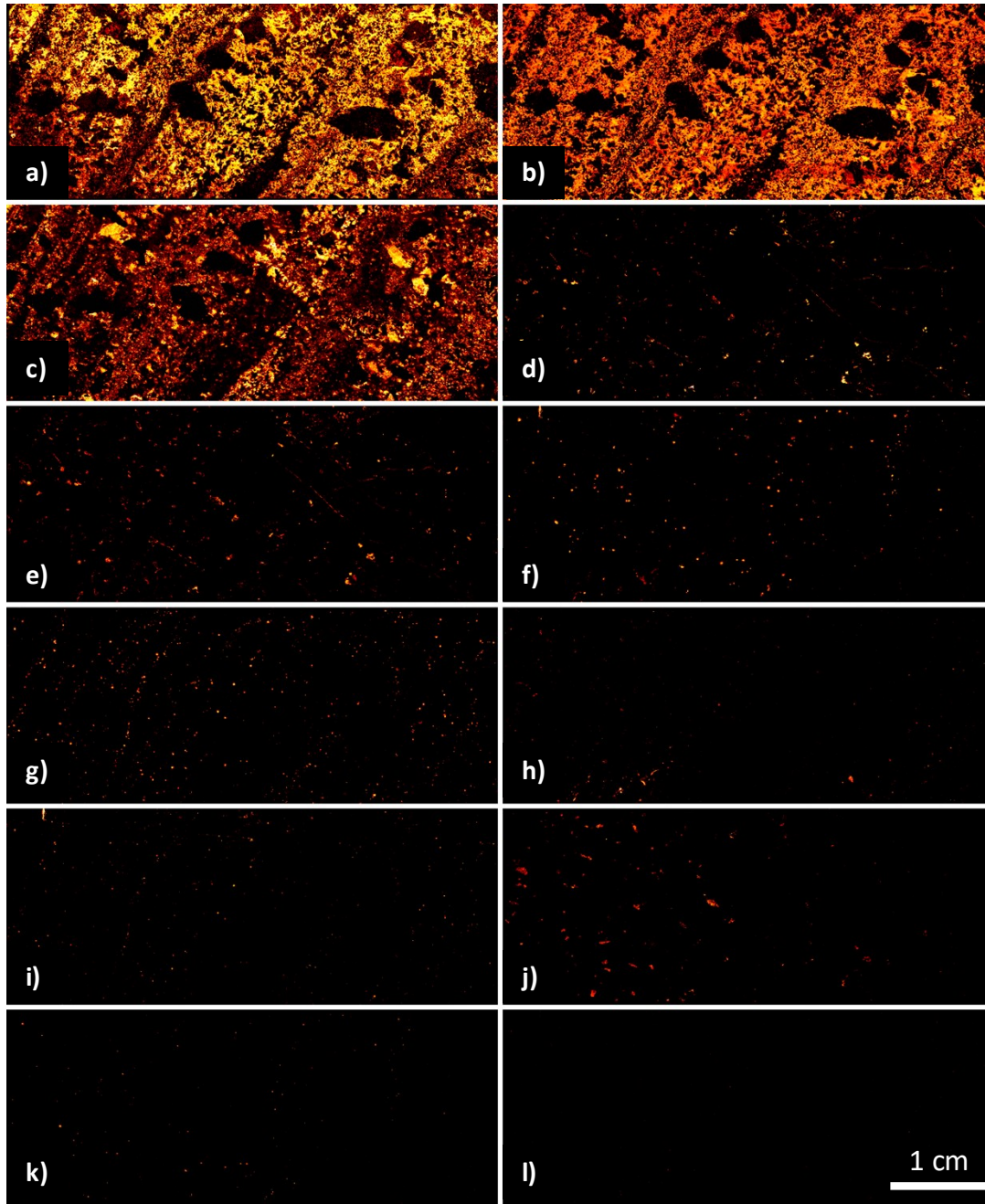


Figure SP 1. Elemental maps for a) Mg II $_{279 \text{ nm}}$, b) Rb I $_{780 \text{ nm}}$, c) Na I $_{819 \text{ nm}}$, d) Ca II $_{318 \text{ nm}}$, e) Sr II $_{346 \text{ nm}}$, f) Zn $_{334 \text{ nm}}$, g) Zr $_{350 \text{ nm}}$, h) Fe I $_{302 \text{ nm}}$, i) Cu $_{327 \text{ nm}}$, j) P I $_{353 \text{ nm}}$, k) Mn II $_{293 \text{ nm}}$, l) Ti II $_{336 \text{ nm}}$

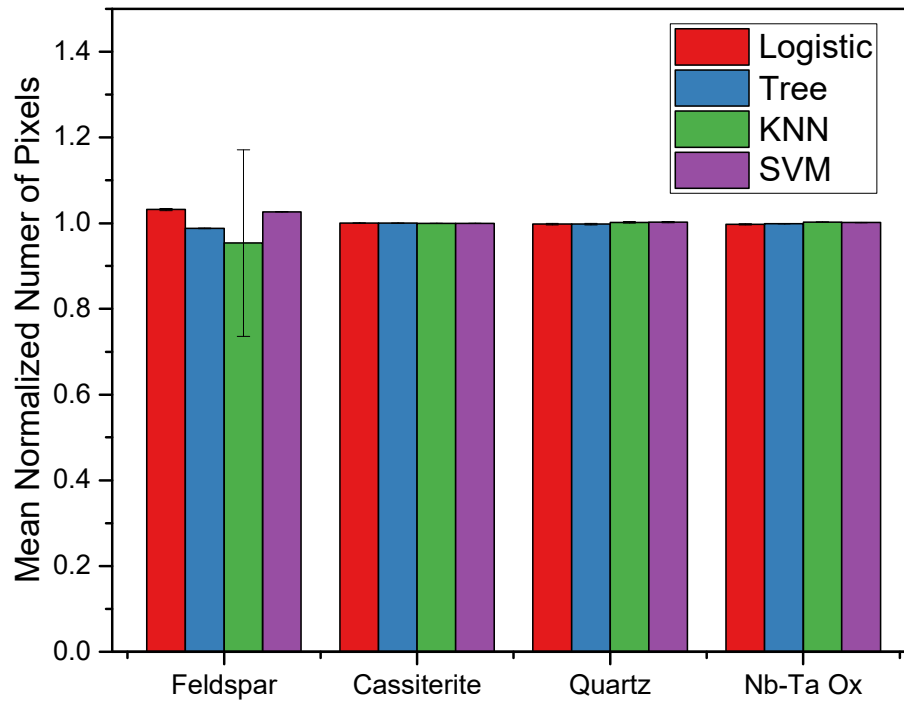


Figure SP 2. Variability of the predicted pixel percentage relative to the mean (set to 1) with respect to the number of pixels attributed to each mineral phase independently.